Life Science Informatics Publications
Research Journal of Life Sciences, Bioinformatics, Pharmaceutical and Chemical Sciences
Journal Home page http://www.rjlbpcs.com/
RJLBPCS
ISSN 2454-6348

Original Research Article **DOI: 10.26479/2018.0404.01**

EXPLORING THE SELECTIVITY OF LIGANDS WITH BCL-6 PROTEIN: A MOLECULAR DOCKING AND DYNAMICS SIMULATION APPROACH

Felisa Parmar[1*], Chirag Patel[2], Hyacinth Highland[1], Himanshu Pandya[2], Linz- Buoy George[1]

1. Department of Zoology, Biomedical Technology and Human Genetics, University School of Sciences, Gujarat University, Ahmedabad, India.
2. Department of Bioinformatics, Applied Botany Centre (ABC), University School of Sciences, Gujarat University, Ahmedabad, India.

ABSTRACT: Initially BCL-6 (B Cell Lymphoma-6) was discovered as an oncogene in B-cell lymphomas, where it drives the malignant phenotype by repressing cell proliferation, DNA damage checkpoints and blocking B-cell terminal differentiation. BCL-6 brings about its effects by binding to several of target genes and then repressing these genes by recruiting several different chromatin-modifying corepressor complexes. Structural characterization of BCL6- corepressor complexes suggested that BCL-6 might be a druggable target. A number of compounds have been designed to bind to BCL-6 and block corepressor recruitment. These compounds, based on peptide or small-molecule scaffolds, can potently block BCL-6 repression of target genes and kill lymphoma cells. The present investigation was an attempt to elucidate efficacy analysis of phytocompounds selected from three plants *Phyllanthus fraternus*, *Mimosa pudica* and *Alstonia scholaris* as antiproliferative agents.

KEYWORDS: BCL-6; L-Mimosine; Kaempferol; Molecular Docking; Molecular Dynamics

Corresponding Author: Felisa Parmar*
Department of Zoology, Biomedical Technology and Human Genetics, University School of Sciences, Gujarat University, Ahmedabad, India.
Email Address: felisaparmar@yahoo.com

1. INTRODUCTION

Development of a drug is a costly, labourious and protracted, where several years are required for a drug to reach the market [1]. Computational techniques have been applied in various drug development studies to attenuate time and costs. By employing computational techniques, many studies have successfully discovered novel therapeutic compounds [2-5]. Natural products are produced by living organisms, such as bacteria, molds, plants and animals, and have been optimized to bind numerous biological macromolecules [6]. Therefore, natural products often prove to be good precursors for selection of lead compounds [7, 8] and for designing good drug candidates [9]. Compared to synthetic compounds, natural products have favorable absorption and metabolism in human body with low toxicity [10]. Natural products are today, choice sources for new drugs [11]. In this study, we aimed to explore the interaction between natural products and protein targets to identify potential ligand-protein inhibition. In drug discovery, computational methods are classified as structure-based drug discovery (SBDD) [12] or ligand-based drug discovery (LBDD) [13, 14]. The SBDD method generally requires target structure information, such as X-ray structure data. In contrast, the LBDD method requires ligand structure information with experimental results. Molecular dynamics (MD) simulation, which can capture the intracellular dynamics of biomolecules at atomic scale resolution, is a powerful computation tool for investigating protein-inhibitor interactions in SBDD. This simulation accounts for protein flexibility using Newtonian principles and has been applied to various biomolecules, such as nucleic acid, biomembranes and proteins [15-24]. B-cell lymphoma 6 (BCL6) protein, is a transcriptional factor, that belongs to the bric-a-brac, tramtrack, broad complex/poxvirus zinc finger (BTB/POZ) family proteins. It possesses BTB, RD2 and zinc finger domains and interacts with three corepressors, i.e., BCoR, SMRT and NCoR. It expresses in lymphocytes and regulates the differentiation and proliferation of lymphocytes [25]. BCL6 controls B cell activation, differentiation, susceptibility to DNA damage, and apoptosis during the proliferative phase of the germinal centers (GC) reaction. BCL6 is expressed in all GC-derived malignancies, including Burkitt's lymphoma (BL), Follicular lymphoma (FL), Diffuse large B-cell lymphomas (DLBCL), and a subset of Hodgkin lymphoma [26]. Direct targeting of BCL6 [27] may represent a strategy to complement other therapeutic approaches aiming to the induction of apoptosis, activation, and/ or differentiation.

2. MATERIALS AND METHODS

2.1 Molecular Dynamics:

2.1.1 Preparation of protein target structure and ligands:

Total 80 phytocompounds were selected from three plants, *Mimosa pudica*, *Phyllanthus fraternus* and *Alstonia scholaris* and retrieved from PubChem database (Table 1). The X-ray

crystal structure of B cell lymphoma proteins were retrieved from the Research Collaboratory for Structural Bio-informatics (RCSB) (http://www.pdb.org/) protein data bank under the PDB ID: 1R29, 5N1X, 5N1Z, 5N20, 5N21, 5X4M, 5X4N and 5X4Q. The 3D structure of selected ligands, Cassiaoccidentalin B, Kaempferol and L-Mimosine, were retrieved in structure data format (SDF) from PubChem (CID- 44257724, 5280863, and 5280863 respectively). YASARA software was used to evaluate molecular docking. For molecular docking study, certain parameters like removal of water, chain selection, and energy minimization were performed by Amber03 force field [28]. Dock poses, docking energy and interacting amino acid residues were analyzed for the prediction of binding affinity and it relies on below equation:

$$\Delta G = \Delta GvdW + \Delta GHbond + \Delta Gelec + \Delta Gtor + \Delta Gdesolv$$

Where,

ΔGvdW = van der Waals term for docking energy

ΔGHbond = H bonding term for docking energy

ΔGelec = electrostatic term for docking energy

ΔGtor = torsional free energy term for ligand when the ligand transits from unbound to bound state

ΔGdesolv = desolvation term for docking energy

Table 1: Phytocompounds selected from the three plants

Ascorbic acid	Mimosine	Scholaricine
Niranthin	Luteolin	Rhazimanine
Hinokinin	Isoquercitin	19-Epischolaricine
Hypophyllanthin	Avicularin	N-methylscholaricine
Phyllanthin	Apigenin-7-O-glucoside	N-methylburnamine
Urinatetralin	Cassiaoccidentalin Beta	Vallesamine N-oxide
Catechin	Orientin	Scholarine N-oxide
Catechin-3-O-gallate	Isoorientin	Picrinine
Gallocatechin	Citric acid	Angustilobine B
Gallocatechin-3-O-gallate	Clorogenic acid	Losbanine
Astragalin	Cafeic acid	Tubotaiwine
Nirurin	Genistein	Lagunamine
Nirurinetin	Naringenin	Ursolic acid
Quercitrin	Vitamin E	Cycloeucalenol
Quercetin	Myo-inositol	Alpha-amyrin acetate
Rutin	Squalene	Beta –sitosterol

Kaempferol	8,11,14-Eicosatrienoic acid	alpha-tocopherol
Dotriacontanoic acid	9,12-Octadecadienoic acid	Dibutylphthalate
Heptacosanoic acid	Hexadecadienoic acid	Isorhamnetin
Linoleic acid	alpha-Spinasterol	Xylobovide
Linolenic acid	Gallic acid	Fusaric acid
Ricinoleic acid	Ellagic acid	Alschomine
Cholesterol	Lupeol	E-alstoscholarine
Phyllanthine	Phytol	Lauric acid
Securinine	Behinic acid	Myristic acid
Triacontanol	Arachidic acid	Palmitic acid
Niruriside		Linolenic acid

Table 2: Different forms of B-Cell Lymphoma 6 (BCL6) BTB Domain

1. 1R29- Crystal Structure of the B-Cell Lymphoma 6 (BCL6) BTB Domain to 1.3 Angstrom 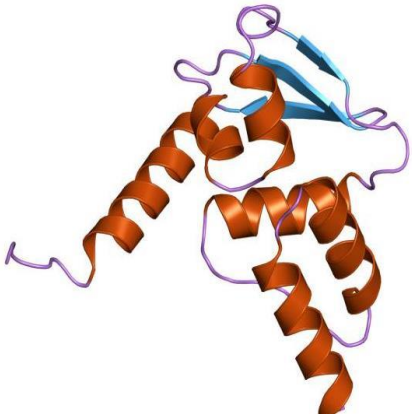	The crystal structure of B-Cell Lymphoma 6 (BCL6) BTB Domain was retrieved from PDB database with the PDB ID 1R29 which belongs to Alpha and Beta proteins, contains one chain having 1.3 Ǻ with 127 amino acids and extracted by X-ray diffraction method.
2. 5N1X- Crystal structure of the BCL6 BTB domain in complex with pyrazolo-pyrimidine ligand 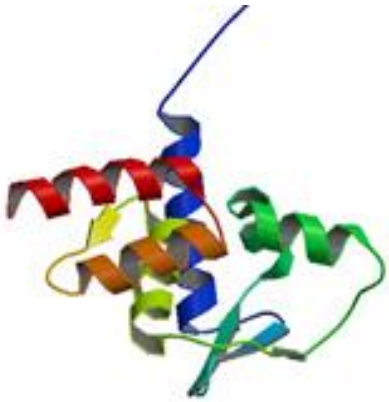	The crystal structure of B-Cell Lymphoma 6 (BCL6) BTB Domain was retrieved from PDB database with the PDB ID 5N1X which contains one chain having 1.72 Ǻ with 121 amino acids and extracted by X-ray diffraction method.

3. 5N1Z- Crystal structure of the BCL6 BTB domain in complex with pyrazolo-pyrimidine macrocyclic ligand 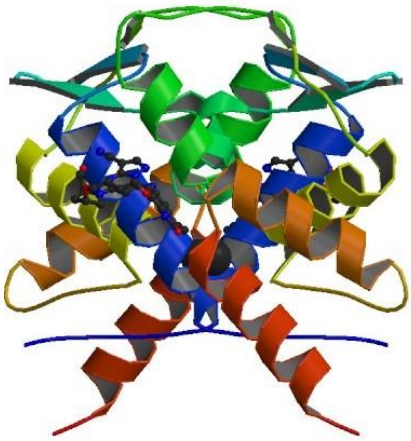	The crystal structure of B-Cell Lymphoma 6 (BCL6) BTB Domain was retrieved from PDB database with the PDB ID 5N1Z which contains one chain having 1.81 Å with 123 amino acids and extracted by X-ray diffraction method.
4. 5N20- Crystal structure of the BCL6 BTB domain in complex with pyrazolo-pyrimidine ligand 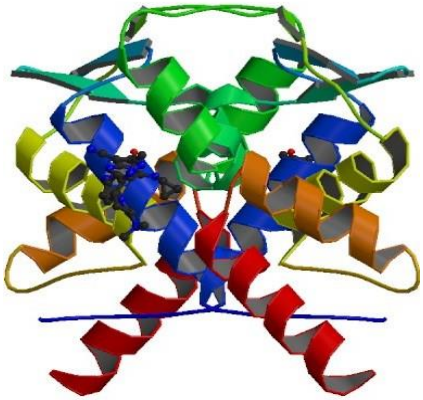	The crystal structure of B-Cell lymphoma 6 (BCL-6) BTB Domain was retrieved from PDB database with the PDB ID 5N20 which contain one chain having 1.38 Å with 123 amino acids and extracted by X-ray diffraction method.
5. 5N21 - Crystal structure of the BCL6 BTB domain in complex with pyrazolo-pyrimidine ligand 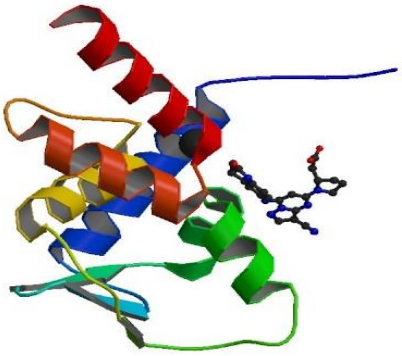	The crystal structure of B-Cell Lymphoma 6 (BCL6) BTB Domain was retrieved from PDB database with the PDB ID 5N21 which belongs to Alpha and beta proteins, contains one chain having 1.58 Å with 122 amino acids and extracted by X-ray diffraction method.

6. 5X4M- Crystal structure of the BCL6 BTB domain in complex with Compound 1 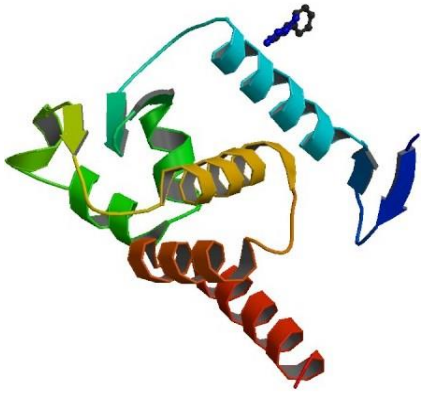	The crystal structure of B-Cell Lymphoma 6 (BCL6) BTB Domain was retrieved from PDB database with the PDB ID 5X4M which belongs to Alpha protein, contains one chain having 1.65 Ǻ with 141 amino acids and extracted by X-ray diffraction method.
7. 5X4N- Crystal structure of the BCL6 BTB domain in complex with Compound 4 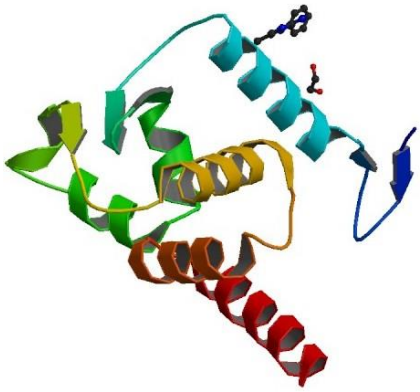	The crystal structure of B-Cell Lymphoma 6 (BCL6) BTB Domain was retrieved from PDB database with the PDB ID 5X4N which belongs to Alpha protein, contains a chain having 1.94 Ǻ with 141 amino acids and extracted by X-ray diffraction method.
8. 5X4Q - Crystal structure of the BCL6 BTB domain in complex with Compound 7 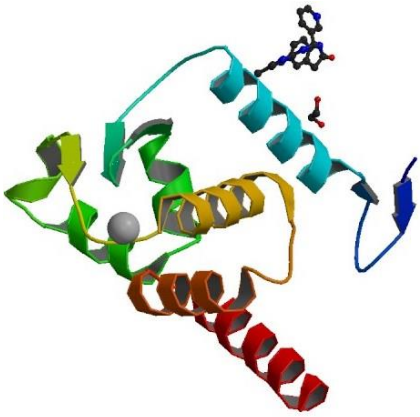	The crystal structure of B-Cell Lymphoma 6 (BCL6) BTB Domain was retrieved from PDB database with the PDB ID 5X4Q which belongs to Alpha protein, contains a chain having 2.0 Ǻ with 141 amino acids and extracted by X-ray diffraction method.

2.2 Molecular Dynamics Simulations:

Molecular dynamics simulation has been performed for conformational changes as well as for the binding stability of the designed ligand in complex with BCL-6 protein. Molecular docking was performed for 3 protein-ligand docked complexes. In addition, we have also carried out molecular dynamics simulation to check the structural change and stability of ligand, whether it retains stability with all proteins or not. The removal of water molecules and optimization have been carried out by using (Y) AMBER force field [29], acid dissociation constant (pKa), and density 0.997g L^{-1} set as per the YASARA structure software to neutralize the system. Then it was subjected to energy minimization by using steepest gradient approach (100 cycles). According to the software parameters force constant has been kept at 1000 KJ mol-1 nm-2, while number of atoms N, pressure P, and temperature T were stored to standard level including temperature of 1 bar using Berendsen thermosat [30] and barostat [31] respectively. By using Protein-Ligand Interaction Profiler 1.2.0 program, the protein ligand interaction patterns obtained from the averaged conformations, were graphically illustrated.

3. RESULTS AND DISCUSSION

Table 3: Docking result analysis of Cassiaoccidentalin B compound with all the selected BCL-6 protein structures

Proteins	Binding Energy [kcal/mol]	Contacting receptor residues
1R29	7.494	LEU A 19 MET A 51 ALA A 52 CYS A 53 SER A 54 GLY A 55 TYR A 58 PHE A 89 MET A 90 SER A 93 GLN A 113 MET A 114 GLU A 115 HIS A 116 VAL A 117
5N1X	8.683	ASN A 21 ARG A 24 ARG A 28 MET B 51 ALA B 52 CYS B 53 SER B 54 GLY B 55 TYR B 58 GLU C 41 PHE C 43 PRO C 80 GLU C 81 ASN C 84 ILE C 85 ARG C 98 ASN C 101
5N1Z	6.953	ALA A 52 CYS A 53 GLY A 55 TYR A 58 SER A 59 PHE A 89 MET A 90 GLN A 113 MET A 114 GLU A 115 HIS A 116 VAL A 117
5N20	7.348	ASN A 23 ARG A 26 SER A 27 ASP A 29 THR A 32 ARG A 40 GLU A 41 GLN A 42 PHE A 43 ARG A 44 ASN A 84 LEU A 87 ASP A 88
5N21	8.053	ASP A 29 LEU A 31 THR A 32 ASP A 33 ARG A 44 LYS A 47 ASN A 68 SER A 70 LEU B 31 ASP B 33 LYS B 47 ARG B 67 ASN B 68 SER B 70

5X4M	7.432	LEU A 19 MET A 51 ALA A 52 CYS A 53 SER A 54 GLY A 55 TYR A 58 PHE A 89 MET A 90 SER A 93 GLN A 113 MET A 114 GLU A 115 HIS A 116 VAL A 117
5X4N	6.316	ARG A 26 SER A 27 ARG A 28 ASP A 29 VAL A 35 GLU A 41 GLN A 42 PHE A 43 ARG A 44 PRO A 80 GLU A 81 CYS A 84 ASP A 88 ARG A 98
5X4Q	7.669	LEU A 19 MET A 51 ALA A 52 CYS A 53 SER A 54 GLY A 55 TYR A 58 PHE A 89 MET A 90 SER A 93 GLN A 113 MET A 114 GLU A 115 HIS A 116 VAL A 117

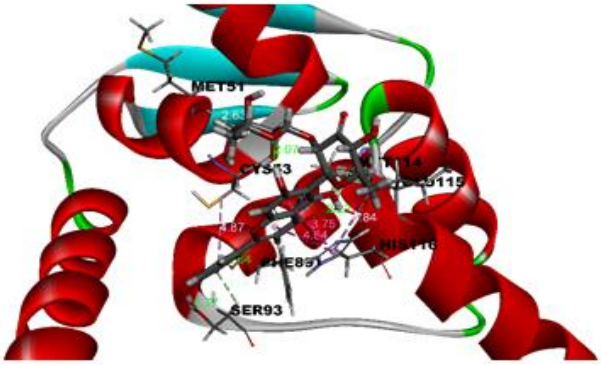

(a) Dock pose of 1R29 with ligand- Cassiaoccidentalin B in 2-D form.

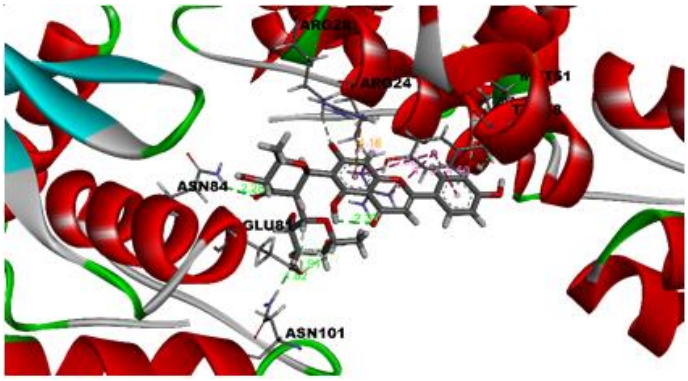

(b) Dock pose of 5N1X with ligand- Cassiaoccidentalin B in 2-D form.

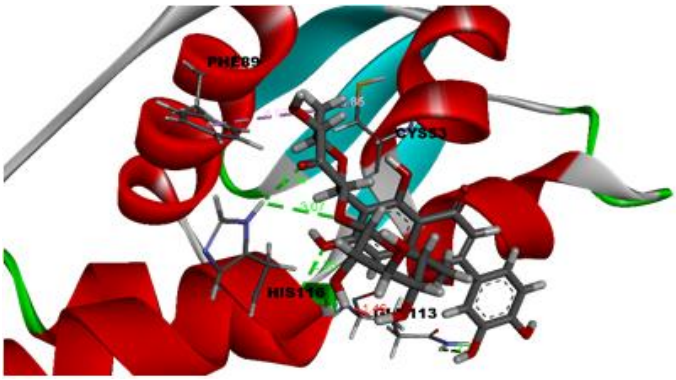

(c) Dock pose of 5N1Z with ligand- Cassiaoccidentalin B in 2-D form.

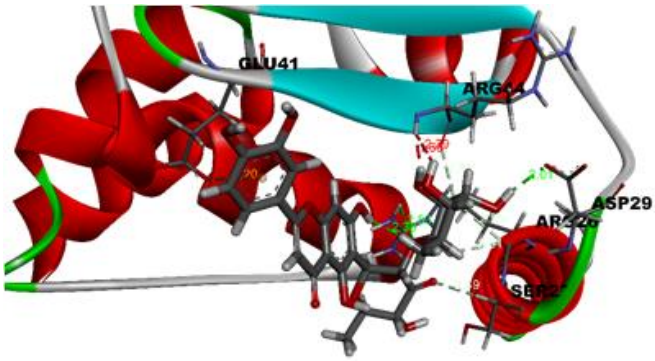

(d) Dock pose of 5N20 with ligand- Cassiaoccidentalin B in 2-D form.

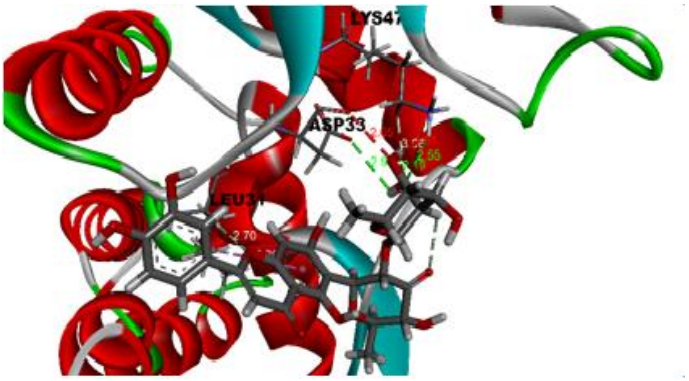

(e) Dock pose of 5N21 with ligand- Cassiaoccidentalin B in 2-D form.

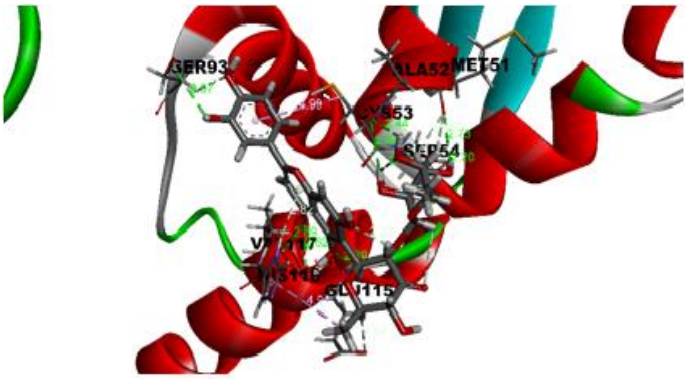

(f) Dock pose of 5X4M with ligand- Cassiaoccidentalin B in 2-D form.

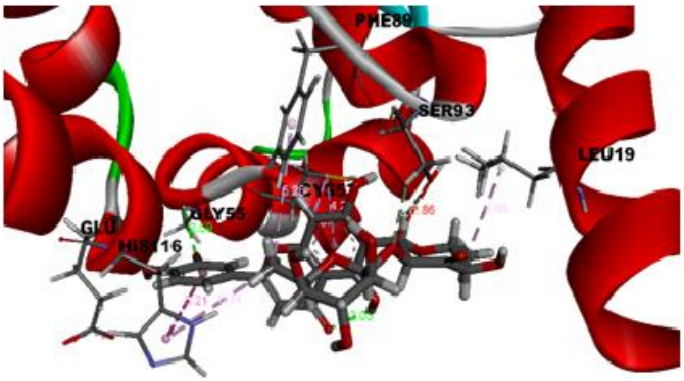

(g) Dock pose of 5X4N with ligand- Cassiaoccidentalin B in 2-D form.

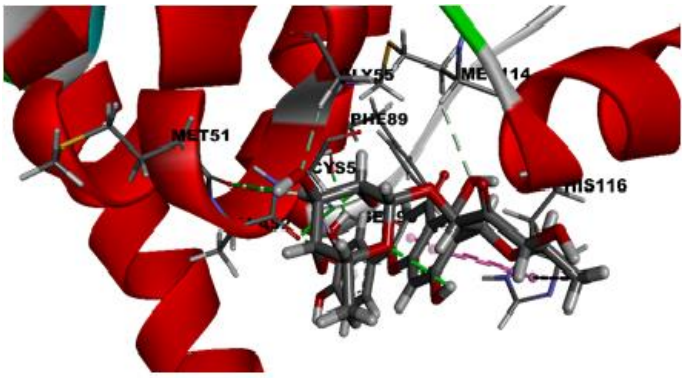

(h) Dock pose of 5X4Q with ligand- Cassiaoccidentalin B in 2-D form.

Figure 1: Dock poses of different forms of BCL-6 protein with Cassiaoccidentalin B in 2-D form

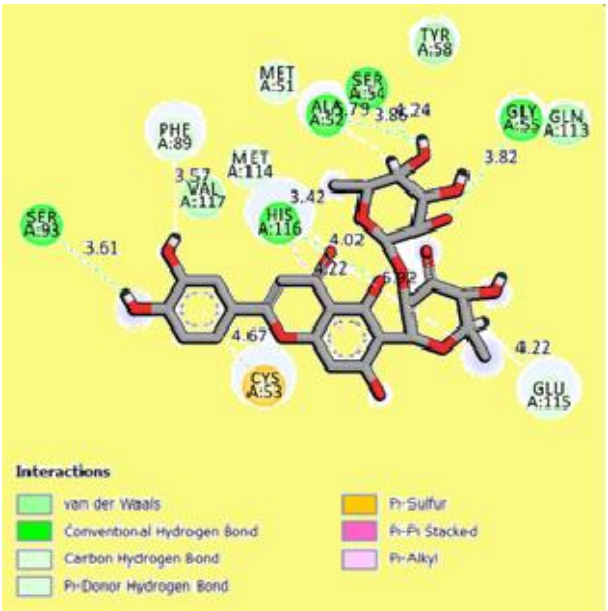

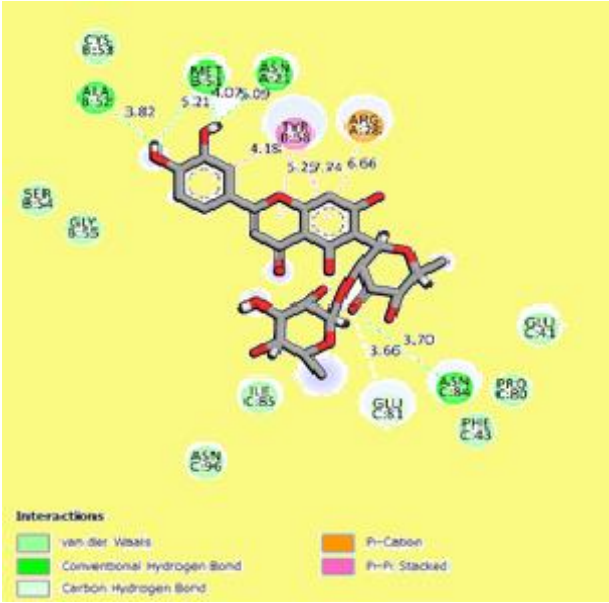

(a): The protein-ligand interaction maps developed from initial molecular dynamics (MD) conformations of prioritized protein target: 1R29-Cassiaoccidentalin B complex.

(b): The protein-ligand interaction maps developed from initial molecular dynamics (MD) conformations of prioritized protein target: 5N1X-Cassiaoccidentalin B complex.

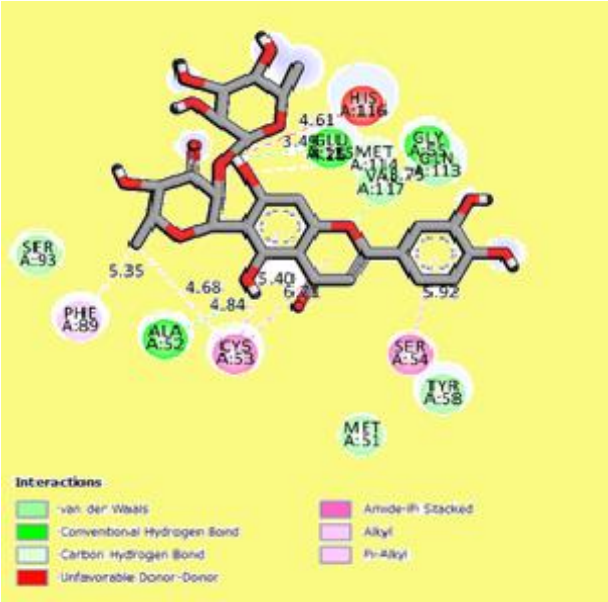

(c): The protein-ligand interaction maps developed from initial molecular dynamics (MD) conformations of prioritized protein target: 5N1Z-Cassiaoccidentalin B complex.

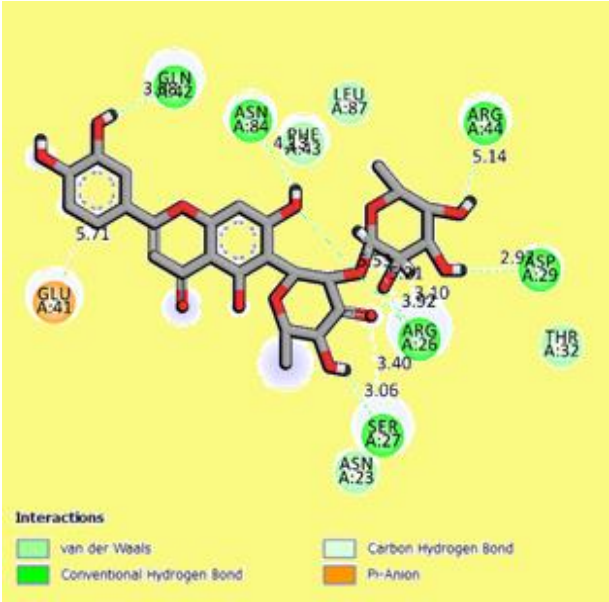

(d): The protein-ligand interaction maps developed from initial molecular dynamics (MD) conformations of prioritized protein target: 5N20-Cassiaoccidentalin B complex.

(e): The protein-ligand interaction maps developed from initial molecular dynamics (MD) conformations of prioritized protein target: 5N21-Cassiaoccidentalin

(f): The protein-ligand interaction maps developed from initial molecular dynamics (MD) conformations of prioritized protein target: 5X4M-

B complex.	Cassiaoccidentalin B complex.
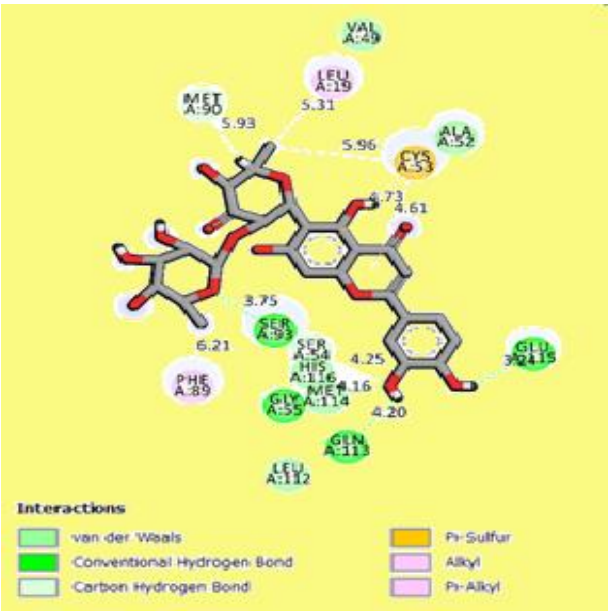 **(g):** The protein-ligand interaction maps developed from initial molecular dynamics (MD) conformations of prioritized protein target: 5X4N-Cassiaoccidentalin B complex.	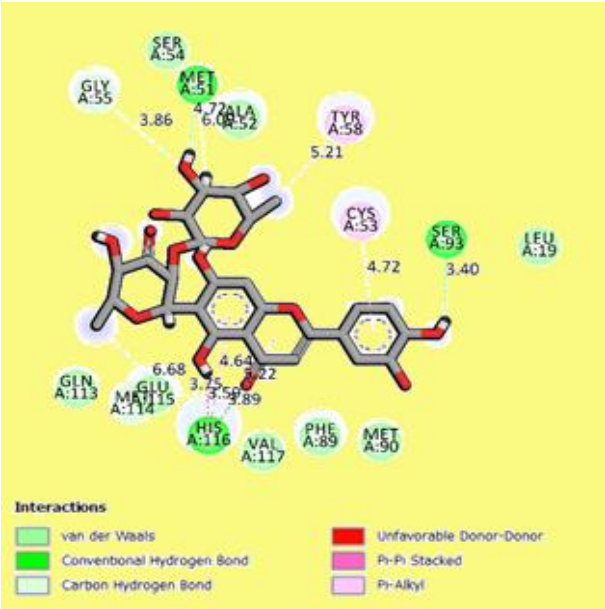 **(h):** The protein-ligand interaction maps developed from initial molecular dynamics (MD) conformations of prioritized protein target: 5X4Q-Cassiaoccidentalin B complex.

Figure 2: The protein-ligand interaction maps developed from initial molecular dynamics (MD) conformation of different forms of BCL-6 protein with Cassiaoccidentalin B

Table 4: Docking result analysis of L-Mimosine and Kaempferol with all proteins

Protein	Ligands	MolDock Score	Steric Interaction
1R29	L-Mimosine	6.092	MET A 51 ALA A 52 CYS A 53 SER A 54 GLY A 55 TYR A 58 GLN A 113 MET A 114 GLU A 115 HIS A 116
	Kaempferol	4.296	MET A 51 ALA A 52 CYS A 53 SER A 54 GLY A 55 TYR A 58 GLN A 113 MET A 114 GLU A 115 HIS A 116 VAL A 117
5N1X	L-Mimosine	7.021	MET A 51 ALA A 52 CYS A 53 SER A 54 GLY A 55 TYR A 58 PHE A 89 GLN A 113 MET A 114 GLU A 115 HIS A 116 VAL A 117 PHE B 11 ARG B 13 HIS B 14 ASP B 17 ASN B 21
	Kaempferol	4.67	ALA C 52 CYS C 53 SER C 54 GLY C 55 PHE C 89 GLN C 113 MET C 114 GLU C 115 HIS C 116 VAL C 117 HIS D 14 ASP D 17 ASN D 21 ARG D 24
5N1Z	L-Mimosine	6.206	LEU A 19 ALA A 52 CYS A 53 SER A 54 GLY A 55 PHE

			A 89 MET A 90 SER A 93 GLN A 113 MET A 114 GLU A 115 HIS A 116 VAL A 117
	Kaempferol	4.423	MET A 51 ALA A 52 CYS A 53 SER A 54 GLY A 55 TYR A 58 SER A 59 GLN A 113 MET A 114 GLU A 115
5N20	L-Mimosine	6.3	MET A 51 ALA A 52 CYS A 53 SER A 54 GLY A 55 TYR A 58 PHE A 89 GLN A 113 MET A 114 GLU A 115 HIS A 116 VAL A 117
	Kaempferol	4.208	MET A 51 ALA A 52 CYS A 53 SER A 54 GLY A 55 TYR A 58 GLN A 113 MET A 114 GLU A 115 HIS A 116
5N21	L-Mimosine	7.376	MET A 51 ALA A 52 CYS A 53 SER A 54 GLY A 55 TYR A 58 PHE A 89 GLN A 113 MET A 114 GLU A 115 HIS A 116 VAL A 117 HIS B 14 ASP B 17 ASN B 21
	Kaempferol	5.552	MET A 51 ALA A 52 CYS A 53 SER A 54 GLY A 55 TYR A 58 PHE A 89 GLN A 113 MET A 114 GLU A 115 HIS A 116 VAL A 117 HIS B 14 ASP B 17 ASN B 21
5X4M	L-Mimosine	6.509	MET A 51 ALA A 52 CYS A 53 SER A 54 GLY A 55 TYR A 58 PHE A 89 GLN A 113 MET A 114 GLU A 115 HIS A 116 VAL A 117
	Kaempferol	4.708	ASN A 23 ARG A 26 SER A 27 ASP A 29 GLN A 42 PHE A 43 ARG A 44 LEU A 87 ASP A 88
5X4N	L-Mimosine	6.004	MET A 51 ALA A 52 CYS A 53 SER A 54 GLY A 55 TYR A 58 PHE A 89 GLN A 113 MET A 114 GLU A 115 HIS A 116 VAL A 117
	Kaempferol	4.29	MET A 51 ALA A 52 CYS A 53 SER A 54 GLY A 55 TYR A 58 GLN A 113 MET A 114 GLU A 115 HIS A 116
5X4Q	L-Mimosine	5.987	MET A 51 ALA A 52 CYS A 53 SER A 54 GLY A 55 TYR A 58 PHE A 89 GLN A 113 MET A 114 GLU A 115 HIS A 116 VAL A 117
	Kaempferol	4.815	MET A 51 ALA A 52 CYS A 53 SER A 54 GLY A 55 TYR A 58 GLN A 113 MET A 114 GLU A 115 HIS A 116 VAL A 117

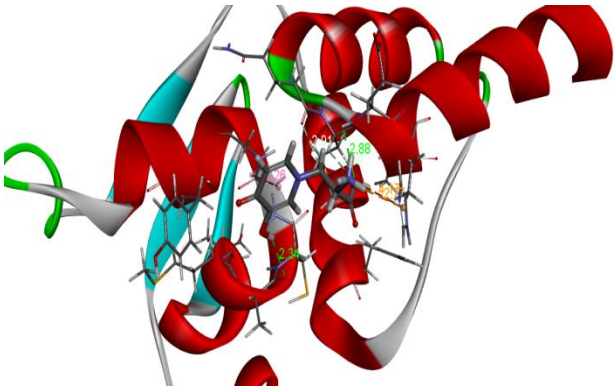

(a): Dock pose of 1R29 with ligand- L-Mimosine in 2-D form.

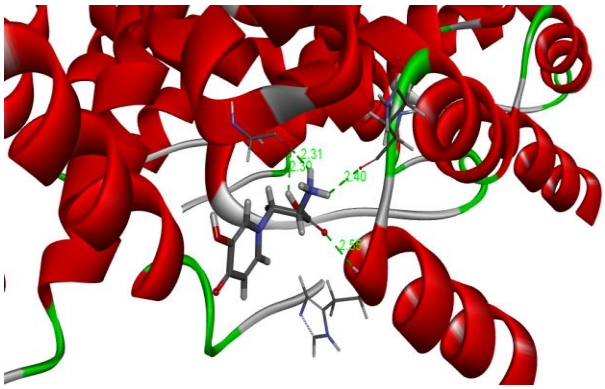

(b): Dock pose of 5N1X with ligand- L-Mimosine in 2-D form.

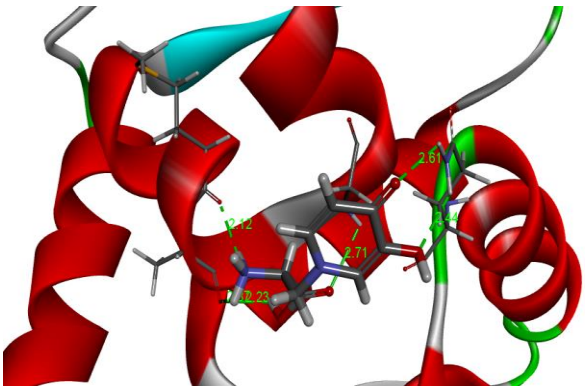

(c): Dock pose of 5N1Z with ligand- L-Mimosine in 2-D form.

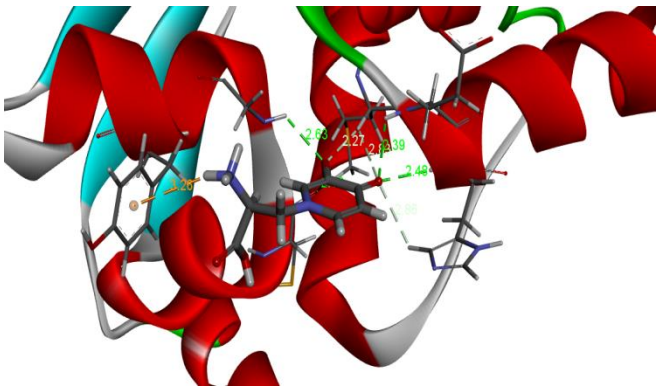

(d): Dock pose of 5N20 with ligand- L-Mimosine in 2-D form.

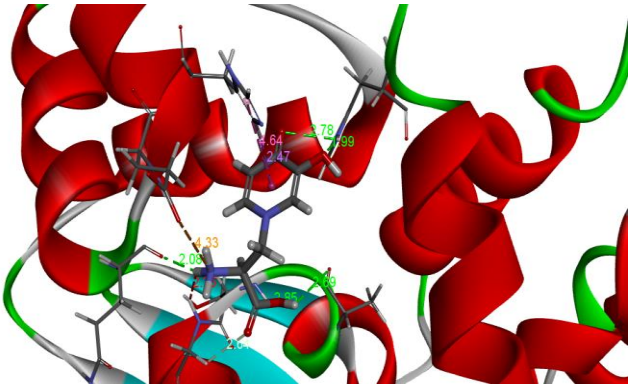

(e): Dock pose of 5N21 with ligand- L-Mimosine in 2-D form.

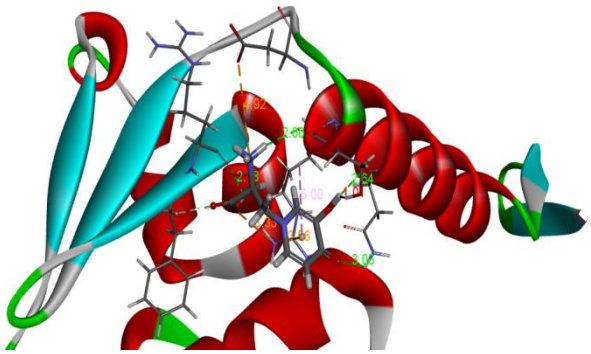

(f): Dock pose of 5X4M with ligand- L-Mimosine in 2-D form.

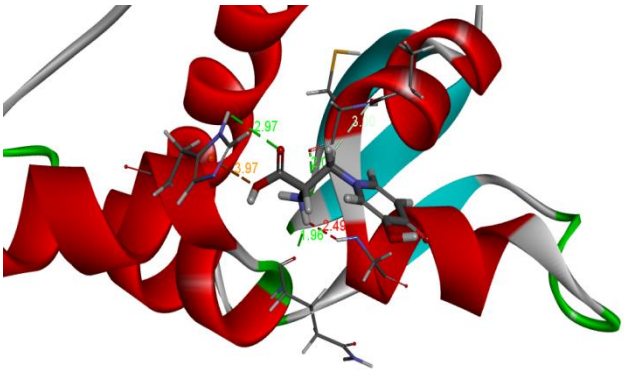

(g): Dock pose of 5X4N with ligand- L-Mimosine in 2-D form.

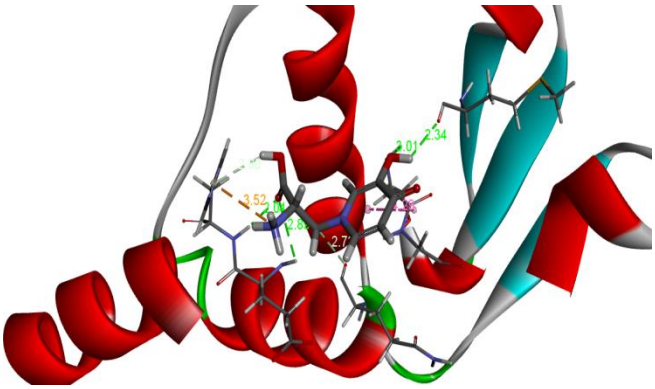

(h): Dock pose of 5X4Q with ligand- L-Mimosine in 2-D form.

Figure 3: Dock poses of different forms of BCL-6 protein with L-Mimosine in 2-D form

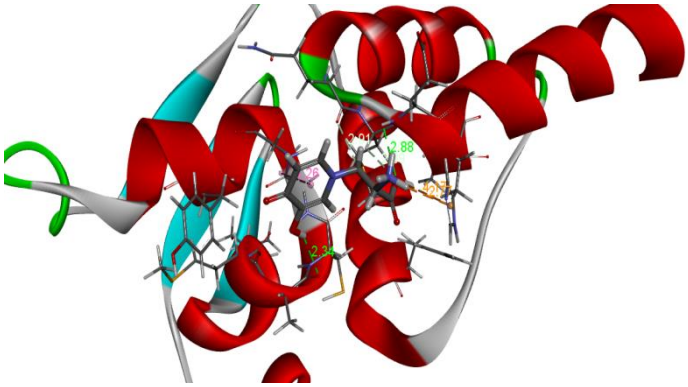

(a): Dock pose of 1R29 with ligand- Kaempferol in 2-D form.

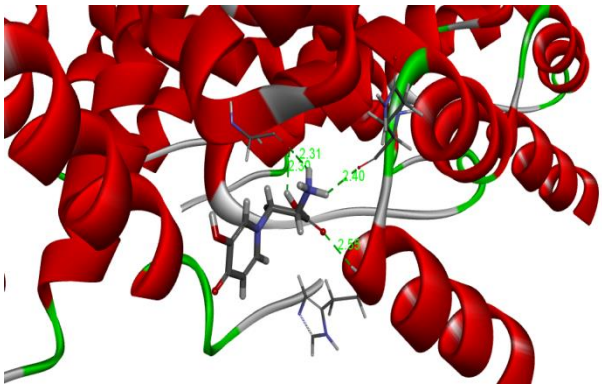

(b): Dock pose of 5N1X with ligand- Kaempferol in 2-D form.

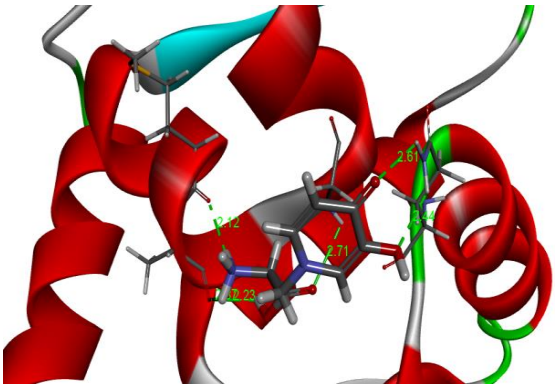

(c): Dock pose of 5N1Z with ligand- Kaempferol in 2-D form.

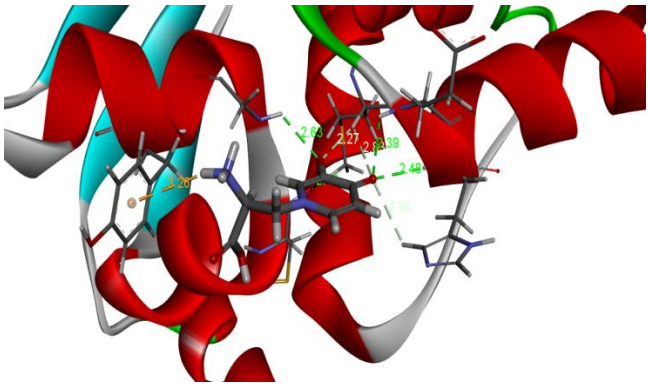

(d): Dock pose of 5N20 with ligand- Kaempferol in 2-D form.

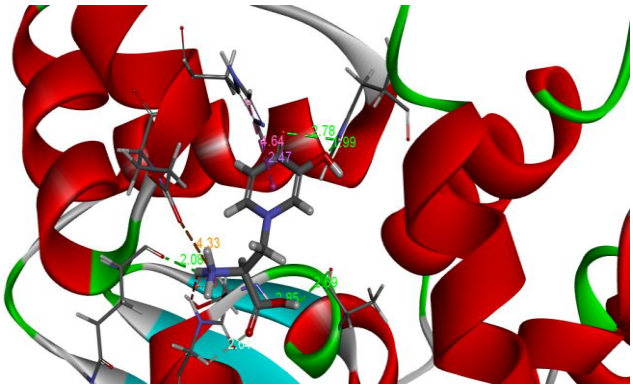

(e): Dock pose of 5N21 with ligand- Kaempferol in 2-D form.

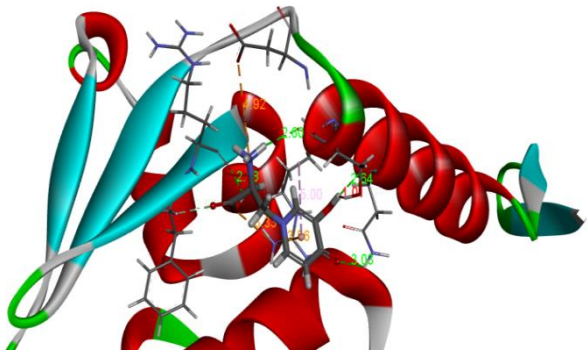

(f): Dock pose of 5X4M with ligand- Kaempferol in 2-D form.

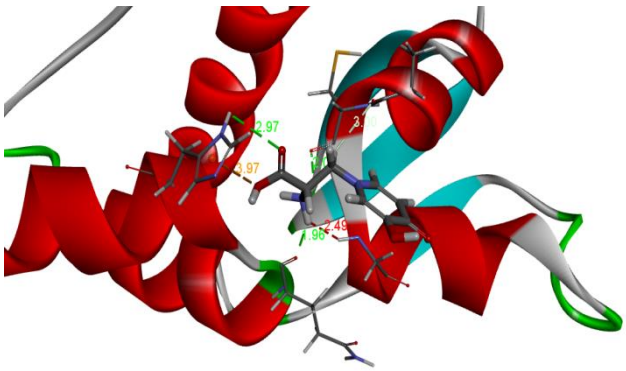

(g): Dock pose of 5X4N with ligand- Kaempferol in 2-D form.

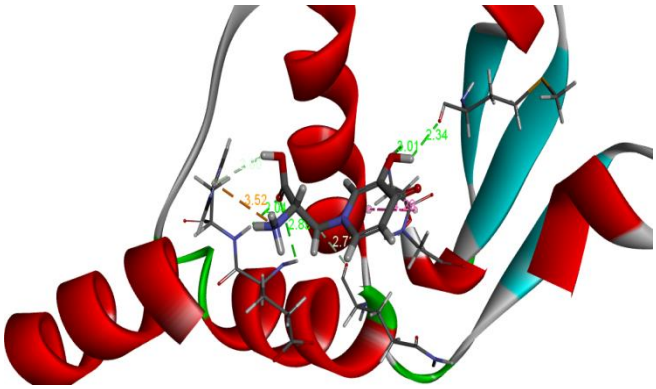

(h): Dock pose of 5X4Q with ligand- Kaempferol in 2-D form.

Figure 4: Dock poses of different forms of BCL-6 protein with Kaempferol in 2-D form

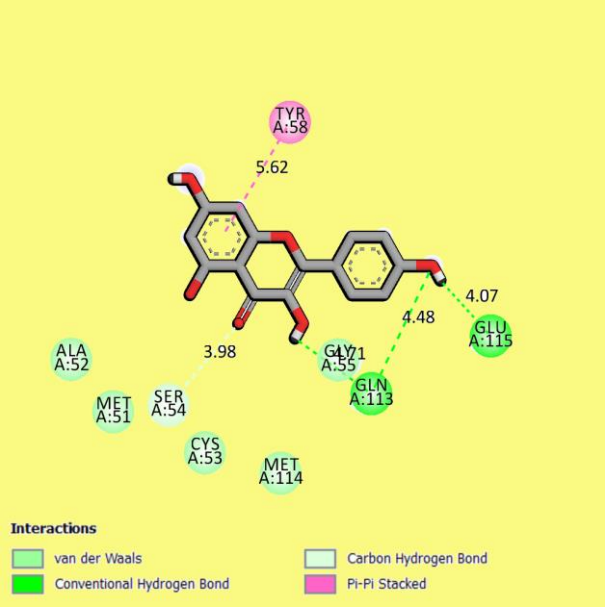

(a): The protein-ligand interaction maps developed

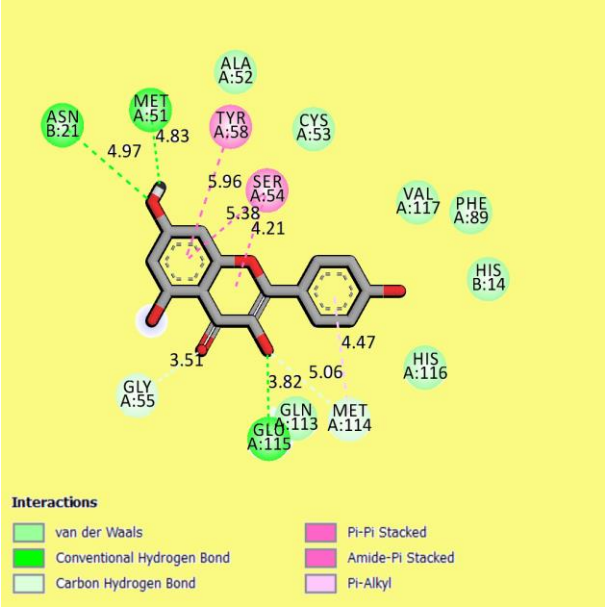

(b): The protein-ligand interaction maps

from initial molecular dynamics (MD) conformations of prioritized protein target: 1R29-L-Mimosine complex.

developed from initial molecular dynamics (MD) conformations of prioritized protein target: 5N1X-L-Mimosine complex.

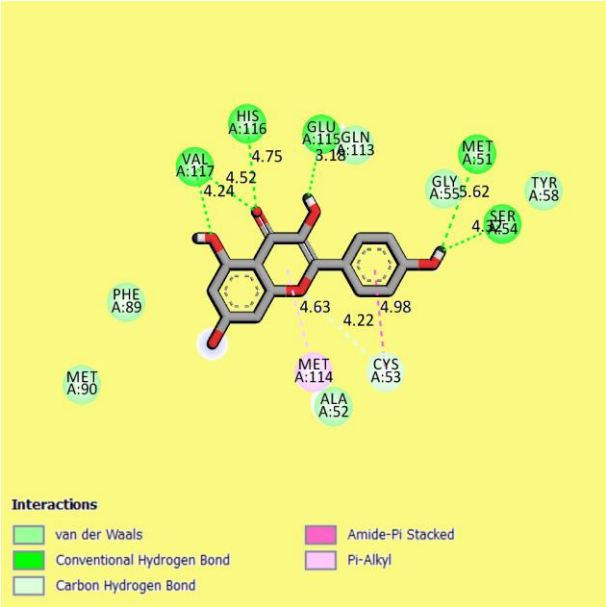

(c): The protein-ligand interaction maps developed from initial molecular dynamics (MD) conformations of prioritized protein target: 5N1Z – L-Mimosine complex.

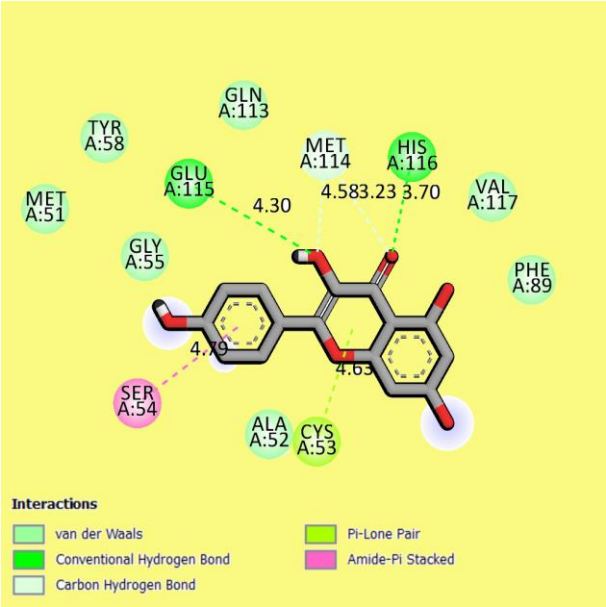

(d): The protein-ligand interaction maps developed from initial molecular dynamics (MD) conformations of prioritized protein target: 5N20-L-Mimosine complex.

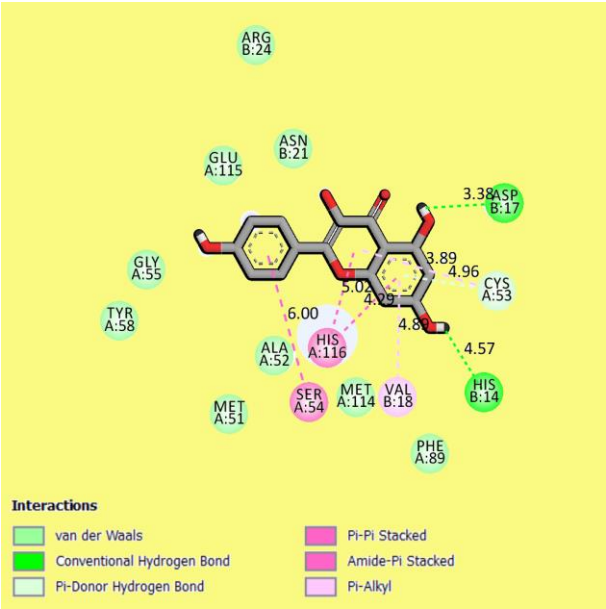

(e): The protein-ligand interaction maps developed from initial molecular dynamics (MD) conformations of prioritized protein target: 5N21-L-Mimosine complex.

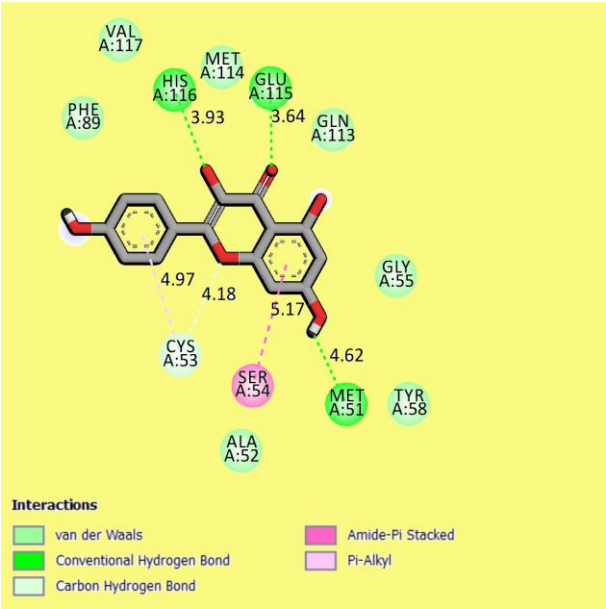

(f): The protein-ligand interaction maps developed from initial molecular dynamics (MD) conformations of prioritized protein target: 5X4M-L-Mimosine complex.

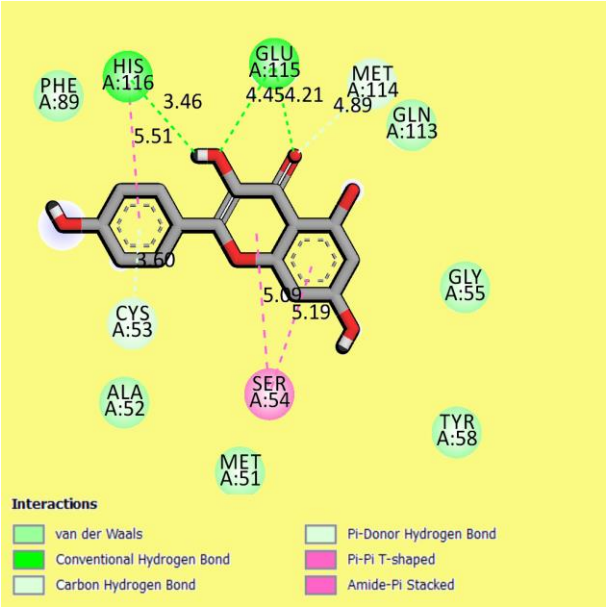

(g): The protein-ligand interaction maps developed from initial molecular dynamics (MD) conformations of prioritized protein target: 5X4N-L-Mimosine complex

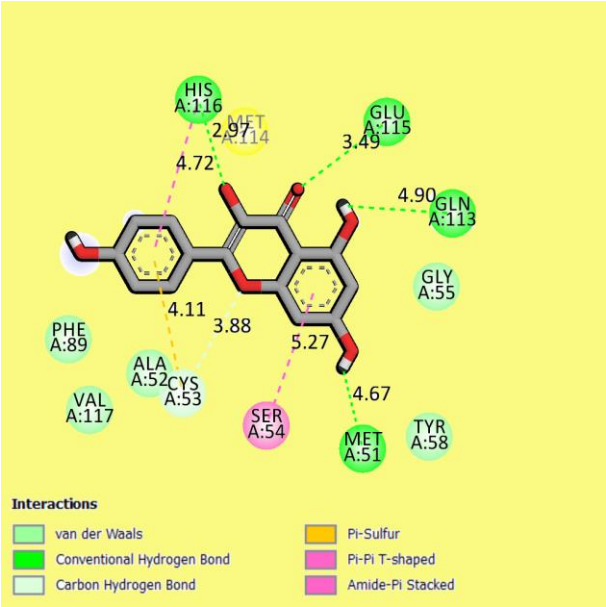

(h): The protein-ligand interaction maps developed from initial molecular dynamics (MD) conformations of prioritized protein target: 5X4Q-L-Mimosine complex.

Figure 5: The protein-ligand interaction maps developed from initial molecular dynamics (MD) conformation of different forms of BCL-6 protein with L-Mimosine

3. RESULTS AND DISCUSSION

3.1 Molecular Docking:

Molecular docking was carried out on protein, B cell lymphoma 6 (BCL-6) BTB Domain with selected phytocompounds (Table-1). Among the different forms of BCL-6 protein (Table 2), 5N1X with Cassiaoccidentalin B and 5N21 was found to be best docked with Kaempferol and L-Mimosine. To study ligand-protein interactions of these phytocompounds, docking study was performed on all the compounds against BCL-6 protein which include hydrogen bonding interactions, hydrophobic interactions, Van der Waals interactions and pi-pi interactions with selected inhibitors. Among all different phytocompounds selected in the present study, Cassiaoccidentalin B, L-Mimosine and Kaempferol were selected for the further analysis of docking studies. According to the results from the molecular docking simulation performed through the YASARA, Cassiaoccidentalin B compound present in *Mimosa pudica* was found as best ligand. It possessed potential binding affinity 8.683 kcal/mol with 5N1X protein. ASN A 21 ARG A 24 ARG A 28 MET B 51 ALA B 52 CYS B 53 SER B 54 GLY B 55 TYR B 58 GLU C 41 PHE C 43 PRO C 80 GLU C 81 ASN C 84 ILE C 85 ARG C 98 ASN C 101 were found as a responsible key residues which revealed the perfect binding of selected protein-ligand complex (Table-3). Along with Cassiaoccidentalin B, L-Mimosine and Kaempferol

molecular docking simulation was performed through the YASARA. L-Mimosine was found to have better docking score as compared to Kaempferol with all the forms of BCL-6 protein. It possessed potential molecular docking score 7.376 kcal/mol with 5N21 protein. Observations indicated that MET A 51 ALA A 52 CYS A 53 SER A 54 GLY A 55 TYR A 58 PHE A 89 GLN A 113 MET A 114 GLU A 115 HIS A 116 VAL A 117 HIS B 14 ASP B 17 ASN B 21 were found as responsible key residues which suggest the perfect binding of selected protein-ligand complex. Kaempferol possessed molecular docking score 5.552 kcal/mol with 5N21 protein. The key residues identified include MET A 51 ALA A 52 CYS A 53 SER A 54 GLY A 55 TYR A 58 PHE A 89 GLN A 113 MET A 114 GLU A 115 HIS A 116 VAL A 117 HIS B 14 ASP B 17 ASN B 21 which indicated the optimum binding of selected protein-ligand complex (Table-4). The docking results of Cassiaoccidentalin B, L-Mimosine and Kaempferol are presented in figures (Figure 1, Figure 3 and Figure 4) respectively.

3.2 Molecular Dynamics (MD):

To understand the stability of BCL-6 - Cassiaoccidentalin B complex and BCL-6 -L-Mimosine complex, we have performed the MD simulations for 1 ns for Cassiaoccidentalin B and L-Mimosine, with the aim to reveal its ability to penetrate through the biomembarne. The MD results of Cassiaoccidentalin B and L-Mimosine are presented in figures (Figure 2 and Figure 5) respectively. The energy of protein ligand complexes calculated over the simulation trajectory showed that BCL-6 developed effective interaction with ligands.

Discussion:

4.1 Molecular Docking

In pharmaceutical research, computational strategies are of great value as they help in the identification and development of novel promising compounds especially by molecular docking methods [32, 33]. Various research groups have applied these methods to screen potential novel compounds against a variety of diseases [34] (Ferreira *et al*., 2015). Plants have long been a very important source of drug and many plants have been screened whether they contain compounds with therapeutic activity [35]. In our present study, we tried to see the interaction of selected phytoconstituents with B cell lymphoma 6 (BCL 6) to inhibit cancer. Docking simulation technique was used for primary analysis of the potential molecular target for the reported anticancer agent. The investigation of the docked ligand permitted us to establish the binding mode of compound involved in this study and confirmed the role as anticancer agent.

4.2 Molecular Dynamics Simulation

BCL6 is a therapeutic target for auto-immune diseases and cancer treatment [36]. Our *in silico* studies had given very promising and interesting results on the effect of B-cell lymphoma 6

(BCL6) protein. Our previous studies have indicated L-Mimosine and Kaempferol both compounds, exhibits antiproliferative activity. Treatment with both the compounds showed antiproliferative effects against Daudi lymphoma cell line [37, 38]. It could be concluded that Cassiaoccidentalin B, L-Mimosine and Kaempferol could be a potential inhibitor of lymphoma cell. Even though, further role of these compounds and their exact mechanism of action remain to be explored.

4. CONCLUSION

Understanding of protein-ligand interactions is important for designing target-selective ligands. In this study, we applied an approach that combined Molecular docking and MD simulation to improve the current understanding of the selectivity of cassioaccidentalin, L-Mimosine and Kaempferol for BCL-6. In this study the docking simulation technique was used preliminarily to investigate the potential molecular target(s) for the reported anticancer agents from natural plant products. The analysis of the best docked ligands permitted us to know the binding mode of compounds involved in this study and confirm the role as anticancer agent. Binding energies of the protein-ligand interactions are important to describe how fit the ligand binds to the macromolecule. The obtained results are useful to understand the structural features required to enhance the inhibitory activities. Without X-ray structures, it is difficult to compare interactions between protein-ligand complexes of interest. Protein-ligand complex modeling, as applied in this study, at least enables comparison of interaction; it does not explain selectivity, stable interaction between protein and ligand could be clarified. Therefore, MD simulation is a powerful tool for elucidating the dynamics of protein-ligand interactions and to support drug design. The insights obtained from the MD simulations may be useful for designing new selective BCL-6 ligands.

5. ACKNOWLEDGEMENT

The authors gratefully acknowledge the Department of Botany, Bioinformatics and Climate Change Impacts Management, Gujarat University for providing an opportunity to access the bioinformatics research facilities. Ms. Felisa Parmar acknowledges financial assistance from University Grants Commission (UGC), Govt. of India as in the form of Maulana Azad National Fellowship (MANF).

6. CONFLICT OF INTEREST

The authors wish to state that there is no conflict of interest associated with the study.

REFERENCES

1. Leelananda SP and Lindert S. Computational methods in drug discovery. Beilstein J Org. Chem. 2016;12:2694–2718.
2. Yoshino R, Yasuo N, Inaoka DK, Hagiwara Y, Ohno K, Orita M et al. Pharmacophore modeling for anti-chagas drug design using the fragment molecular orbital method. PLoS One 10 2015 e0125829.
3. Yoshino R, Yasuo N, Hagiwara Y, Ishida T, Inaoka DK, Amano Y et al. *In silico, in vitro*, X-ray crystallography, and integrated strategies for discover ingspermidine synthase inhibitors for Chagas disease. Sci. Rep. 2017;7:6666.
4. Chiba S, Ikeda K, Ishida T, Gromiha MM, Taguchi YH, Iwadate M et al. Identification of potential inhibitors based on compound proposal contest: tyrosine-protein kinase Yes as a target. Sci Rep. 2015;5;17209.
5. Chiba S, Ishida T, Ikeda K, Mochizuki M, Teramoto R, Taguchi Y et al. An iterative compound screening contest method for identifying target protein inhibitors using the tyrosine-protein kinase Yes. Sci Rep. 2017;7:12038.
6. KhannaV and Ranganathan S. Structural diversity of biologically interesting datasets: A scaffold analysis approach. J. Cheminform. 2011;3:30.
7. Patridge E, Gareiss P, Kinch MS and Hoyer D. An analysis of FDA-approved drugs: natural products and their derivatives. Drug Discov Today. 2016;21:204.
8. Muigg P, Rosen J, Bohlin L and Backlund A. *In silico* comparison of marine, terrestrial and synthetic compounds using ChemGPS-NP for navigating chemical space. Phytochem. Rev. 2013;12:449–457.
9. Ertl P, Roggo S and Schuffenhauer A. Natural product-likeness score and its application for prioritization of compound libraries. J. Chem. Inf. Model 2008;48:68–74.
10. Luo F, Gu J, Chen L and Xu X. Systems pharmacology strategies for anticancer drug discovery based on natural products. Mol. Biosyst. 2014;10:1912–1917.
11. Newman DJ and Cragg GM. Natural products as sources of new drugs from 1981 to 2014. J. Nat. Prod. 2016;79: 629–661.
12. Kuntz ID. Structure-based strategies for drug design and discovery. Science. 1992;257: 1078-1082.
13. Guner OF. (Ed.), Pharmacophore perception, development, and use in drug design. Vol. 2, International University Line. 2002.
14. Tropsha A. QSAR in drug discovery. Drug Design: Structure Ligand-Based Approaches. 2010;151–164.

15. Arora K and Brooks CL. Functionally important conformations of the Met20 loop in dihydrofolate reductase are populated by rapid thermal fluctuations. J. Am. Chem. Soc. 2009;131:5642–5647.
16. Sulkowska JI, Noel JK, Onuchic JN. Energy landscape of knotted protein folding. Proc. Natl. Acad. Sci. 2012;109:17783–17788.
17. Nam K, Pu JZ, Karplus M. Trapping the ATP binding state leads to a detailed understanding of the F1-ATPase mechanism. Proc. Natl. Acad. Sci. 2014 ;111:7851–17856.
18. Hayes RL, Noel JK, Mohanty U, Whitford PC, Hennelly SP, Onuchic JN et al. Magnesium fluctuations modulate RNA dynamics in the SAM-I riboswitch. J. Am. Chem. Soc. 2012;134:12043–12053.
19. Yildirim A, Sharma M, Varner BM, Fang L and Feig M. Conformational preferences of DNA in reduced dielectric environments. J. Phys Chem. B. 2014;118:10874–10881.
20. Sekijima M, Motono C, Yamasaki S, Kaneko K and Akiyama Y. Molecular dynamics simulation of dimeric and monomeric forms of human prion protein: insight into dynamics and properties. Biophys. J. 2003;85:1176–1185.
21. Gapsys V, de Groot BL and Briones R. Computational analysis of local membrane properties. J. Comput. Aided Mol. Des. 2013;27:845–858.
22. Ingolfsson HI, Melo MN, Van Eerden FJ, Arnarez C, Lopez CA, Wassenaar TA. Lipid organization of the plasma membrane. J. Am. Chem. Soc. 2014;136:14554–14559.
23. Levine ZA, Venable RM, Watson MC, Lerner MG, Shea JE, Pastor RW et al. Determination of biomembrane bending moduli in fully atomistic simulations. J. Am. Chem. Soc. 2014;136:13582–13585.
24. Sodt AJ, Sandar ML, Gawrisch K, Pastor RW and Lyman E. The molecular structure of the liquid-ordered phase of lipid bilayers. J. Am. Chem. Soc. 2014;136:725–732.
25. Melnick A, Carlile G, Ahmad KF, Kiang CL, Corcoran C, Bardwell V et al. Critical residues within the BTB domain of PLZF and Bcl-6 modulate interaction with corepressors. Mol. Cell. Biol. 2002;22:1804-1818.
26. Basso K and Dalla-Favera R. BCL6: master regulator of the germinal center reaction and key oncogene in B cell lymphomagenesis, In Adv. Immun. 2010;105: 193-210.
27. Cerchietti LC, Yang SN, Shaknovich R, Hatzi K, Polo JM, Chadburn A et al. A peptomimetic inhibitor of BCL6 with potent antilymphoma effects *in vitro* and *in vivo*. Blood. 2009;113:3397–3405.
28. Patel CN, George JJ, Modi KM, Narechania MB, Patel DP, Gonzalez FJ et al. (2017). Pharmacophore-based virtual screening of catechol-o-methyltransferase (COMT) inhibitors to combat Alzheimer's disease. J. Biomol. Strct. Dyn. 2017; 1-20.

29. Krieger E and Vriend G. New ways to boost molecular dynamics simulations. J. Comput. Chem. 2015;36:996-1007.
30. Berendsen HJ, Postma JV, van Gunsteren WF, DiNola ARHJ and Haak JR. Molecular dynamics with coupling to an external bath. J. Chem. Phys. 1984;81:3684-3690
31. Allen MP and Tildesley DJ. Computer simulation of liquids. Clarendon Press, Oxford 1987.
32. Lounnas V, Ritschel T, Kelder J, McGuire R, Bywater RP and Foloppe N. Current progress in structure-based rational drug design marks a new mindset in drug discovery. Comput. Struct. Biotechnol. J. 2013; 5, e201302011.
33. Yuriev E and Ramsland PA. Latest developments in molecular docking: 2010–2011 in review. J. Mol. Recognit. 2013;26:215–239.
34. Ferreira LG, Dos Santos RN, Oliva G and Andricopulo AD. Molecular docking and structure-based drug design strategies. Molecules. 2015;20:13384–13421.
35. Emran TB, Rahman MA, Uddin MMN, Dash R, Hossen MF, Mohiuddin M et al. Molecular docking and inhibition studies on the interactions of Bacopa monnieri's potent phytochemicals against pathogenic *Staphylococcus aureus*. DARU J. Pharmaceutical Sci. 2015;23:26.
36. Kamada Y, Sakai N, Sogabe S, Ida K, Oki H, Sakamoto K et al. Discovery of a B-cell lymphoma 6 Protein–Protein Interaction Inhibitor by a Biophysics-driven Fragment-based Approach. J. Med. Chem. 2017;60:4358-4368.
37. Parmar F, Kushwaha N, Highland H, George L, *In vitro* antioxidant and anticancer activity of *Mimosa pudica* Linn extract and L-Mimosine on Lymphoma Daudi cells. International J. Pharm. Pharma Sci. 2015;7:100-104.
38. Parmar F, Patel C, Highland H, Pandya H and George LB. Antiproliferative Efficacy of Kaempferol on Cultured Daudi Cells: An *In Silico* and *In Vitro* Study. Adv. Biol. 2016 (2016) 1-10.